

Controlling Single-Stage and Quasi-Resonant Flyback Converters for Solar Power Systems

Yasmine Ashraf¹, Noorhan E. Elsobky², Mostafa A. Hamouda³, Mohamed Sabry⁴,
Sahar S. Kaddah⁵, Basem M. Badr^{6*} 

^{1,2,3,4} Electrical Power and Machines Department, Mansoura University, Mansoura, Egypt

⁵ Electrical Engineering Department, Mansoura University, Mansoura, Egypt

⁶ Genesis Robotics and Motion Technologies, Vancouver, British Columbia, Canada

E-mail: bbadr@uvic.ca

Received: December 17, 2020

Revised: February 03, 2021

Accepted: February 08, 2021

Abstract— In this paper, single-stage (SS) and quasi-resonant (QR) flyback converters are designed - for a photovoltaic (PV) array with an output voltage of 17 V - to produce the required output voltage of 24 V. Two control systems are used to control the output voltage of the flyback converters, namely proportional integral derivative (PID) and fuzzy logic controller (FLC). MATLAB/Simulink is used to simulate the output of the PV array and to investigate the performance of the open loop and closed loop PID and FLC systems for the SS and QR flybacks under various solar radiation and load conditions. The obtained results show that while the input power of the converters - coming from the PV array - is varying and for various loads, the output voltage stabilizes successfully to the required voltage. Analysis of the obtained results indicates that the maximum achieved efficiency is 89% and 94% for the designed QR flyback for open loop and closed loop, respectively and that the FLC system for the flybacks achieves the fastest and most stable response for the dynamic PV systems.

Keywords— Photovoltaic system; Single-stage flyback converter; Quasi-resonant flyback converter; Control systems; Fuzzy logic controller.

1. INTRODUCTION

Renewable energy sources are becoming increasingly popular due to various environmental concerns and the need for more energy. They are inherently pollution-free and in their availability continuously free. The photovoltaic (PV) systems are expected to become one of the major energy resources to meet the global energy requirement. In 2010, the use of renewable energy amounted to 1684 million tons of oil equivalent, representing 13% of global demand for primary energy. Wind power, solar PV, and hydropower together made up over 85% of renewables growth. Solar PV electricity generation increased by about 130 TWh globally in 2019, second only to wind in absolute terms, reaching 2.7% of electricity supply. Solar PV's year-on-year growth of 22% far exceeded that of wind power [1, 2].

Power converters are becoming very critical, especially when they are used in any sources of energy generation such as solar PV. Since these PV converters are part of the power conversion infrastructure, any premature failure of such a system will cause the entire system to be defective and must, therefore, be selected appropriately. These power converters need to be selected and optimized to ensure the extreme energy efficiency, reliability, and safety of the total solar PV system needed for different applications. This paper focuses on designing and analyzing flyback converters to provide the required power from a solar panel. The performance and characterization of these converters - investigated in this paper - concern different control schemes and various conditions of the PV systems. The paper also highlights the flyback converters review and brings out a few research results

* Corresponding author

about the performance of different existing flyback converters based on the literature analysis by the authors.

Fig. 1 shows the block diagram of the solar power (PV) system. The general PV system consists of solar panels, power converters, battery charging systems and loads. The connection between the inverters and power converters is bidirectional connection, as the power from the grid can be used to charge the batteries. The proposed PV system of this work is based on single-stage (SS) and quasi-resonant (QR) flyback converters for a solar panel, where these converters and control systems are designed for PV applications. These control systems are proportional integral derivative controller (PID) and fuzzy logic controller (FLC). This paper illustrates a simulation work of the PV designs based on SS and QR flyback converters, where these converters are proposed to generate the required power from a solar panel. These converters are designed to output 24 V from 17 V (output voltage from a solar panel), and the proposed control systems are used to regulate the output voltage of these converters for the loads while the output voltage of the solar panel is varying because of the variant of sun radiation and other factors, as described in section 4.

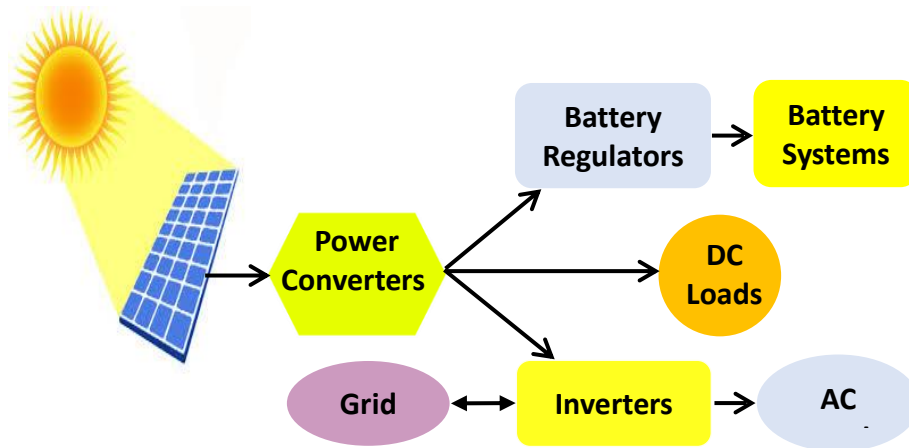


Fig. 1. Block diagram of the solar power system.

This paper is structured as follows: section 1 provides the research motivation for using PV system. Section 2 includes the literature survey of flyback converters in the field of PV applications. Two types of flyback are discussed in section 3, where necessary analytical equations are derived. Section 4 shows the simulation results of the control systems for the flyback converters. The comparative analysis of the flyback converters using the two control techniques is illustrated in section 5. Finally, the conclusions of the paper are drawn in section 6.

2. LITERATURE SURVEY

This section discusses the state of the art in the field of flyback converters for PV applications. K. Raghavendra et al. [3] reviewed and analyzed the most important features of the DC-DC converters along with the maximum power point tracking (MPPT) techniques in the field of solar PV applications. They evaluated the classification of these converters including the flyback converter. They found that the efficiency of the flyback converters can be enhanced by the zero voltage switching (ZVS) operation; soft switching was obtained by employing the clamp circuits along with the resonant-based flyback converters.

J. Gowrishankar et al. [4] modeled PV array for DC-DC flyback converter with asymmetrical output voltage. They designed the circuit as a single input (48 V) with multiple output flyback converters, with which the solar system was fed. They simulated, designed, and built the system using MATLAB and Arduino, where the switching frequency was 65 kHz. The experimental results show that there are 4 different asymmetrical output voltages (6.6 V, 13.2 V, 26.4 V and 52.8 V). G. Chu et al. [5] designed a bidirectional flyback converter based isolated-port differential power processing (DPP) architecture at the submodule level. The bidirectional flyback converters were designed for submodules with both discontinuous conduction mode (DCM) and continuous conduction mode (CCM) for light and heavy load conditions to improve the efficiency. Both simulation and experimental results for an isolated-port DPP regulated 72-cells PV module under various partial shading scenarios were provided. The measured efficiency with the isolated-port DPP structure was 90.2% under severe shading conditions. The measured output power improvement under severe mismatch conditions was high up to 43.1%. U. Yilmaz et al. [6] designed a PV system with incremental conductance (IC) MPPT method applied to the flyback converter under variable temperature (25-50 °C) and irradiance (600-1000 W/m²). In this study, the IC MPPT method was used because it was easy to implement and it showed good performance under variable weather conditions. The system was constructed and analyzed in MATLAB/Simulink, where the MPPT of the PV panel was 75 W and the efficiency of the system was 94%. M. Nasir et al. [7] designed a highly distributed off-grid solar photovoltaic DC microgrid architecture suitable for rural electrification in developing countries. The proposed microgrid architecture consisted of several nano grids capable of the self-sustained generation, storage, and bidirectional flow of power within the microgrid. Bidirectional power flow and distributed voltage droop control were implemented through the duty cycle control of a modified flyback converter. A detailed analysis in terms of power flow, loss and system efficiency was conducted using Newton-Raphson method modified for DC power flow at varying distribution voltages, conductor sizes and schemes of interconnection among the contributing Nano grids. A scaled-down version of the proposed architecture with various power-sharing scenarios was also implemented with a distribution efficiency of 96%. A. Sharma et al. [8] designed a DC-DC flyback converter, where the battery charger and the converter were combined in a single unit with three-port converter topology. Flyback forward converter (1 kW) was employed using MATLAB/Simulink for a three-port topology which has the advantages like large voltage conversion ratio, small input current-ripple, galvanic isolation and high efficiency. PWM and Phase-shifted control strategies were used to transfer the energy to the high voltage output or to the battery. J. H. Lee et al. designed an isolated coupled-inductor integrated DC-DC converter with a non-dissipative snubber to reduce the voltage spike on switches and recycle leakage energy for solar energy applications. The energy in the coupled inductor leakage inductance was recycled via a non-dissipative snubber on the primary side. Experiments were performed using a 200 W solar array simulator, a 24 V solar voltage, and a 200 V output voltage. The experimental results show that the peak efficiency of the proposed converter was about 93.8% [9]. Z. Chen et al. designed DC-DC converters with high-voltage gain with efficiency of 92.5% to 93.5% and low-input current ripple for PV applications. Their model was based on a coupled-inductor boost integrated flyback converter with high-voltage gain and ripple-free input current.

Experimental results show that the designed converter had inherent characteristics of zero input current ripple, less switch voltage stress than the output voltage. The passive lossless snubber circuit recycled the leakage inductor energy and absorbed the switch voltage spike stress, which made the design of the electromagnetic interference (EMI) filter easy [10]. A. Mukherjee designed and simulated flyback micro-inverters for solar energy systems using PSIM software. The main purpose of his design was to improve the efficiency of the harvesting system. He found that the flyback micro-inverter - with a regenerative snubber and the variable switching quasi-resonant ZVS technique - more efficient (more than 1%) than an active clamp ZVS flyback micro-inverter [11]. Y. Zhou designed and implemented a PV converter for DC microgrid with a fast and accurate MPPT strategy using boundary controllers. He concluded that a low-power micro-inverter that uses a flyback converter - instead of a boost converter - gives galvanic isolation and a high boosting ratio by adjusting the high-frequency transformer turns ratio [12]. S. Zengin et al. designed a 200 W two-stage soft-switched flyback micro-inverter to minimize decoupling capacitor value by 10 times. They analyzed and compared the results of the SS flyback micro-inverter and the proposed two-stage design. They found that the efficiency increased from 78% to 88.7% and that the design of a two-stage soft switched flyback micro-inverter requires extra switching elements and passive components, so the cost and the control complexity increase [13]. S. A. Ansari et al. designed a new soft-switching flyback inverter to achieve low output current total harmonic distortion (THD) for PV applications. The inverter consisted of hard switching flyback converter operating in DCM condition with 100 kHz switching frequency and an auxiliary circuit containing a resonant capacitor and resonant inductor. The control schemes were implemented in an ARM-based microcontroller STM32F103C8 development board. The experimental results improved weighted efficiency as well as output current THD (~3.1%) under all load conditions [14]. G. Tan et al. designed a single-phase flyback inverter for PV applications. They used passive and active soft-switching solutions to achieve ZCS and to generate positive and negative output current. The experimental results - based on a laboratory 500 W prototype - showed good output current waveform with nearly unity power factor and low current harmonics. The inverter illustrated the advantages of high power factor, low current distortion, small power decoupling capacitor and soft-switching operation [15]. W. Xiang designed a multi-stage flyback converter for wide input voltage range applications. An intermediate circuit was used with the two flyback stages, where the first stage included the primary winding of the flyback transformer and a switch coupled in series between the midpoint of the intermediate circuit and negative DC terminal. The second stage included second primary windings and a switch coupled in series between the midpoint of the intermediate circuit and positive DC terminal; the two switches operated synchronously. This design was used to reduce voltage stress on the circuit components and to improve efficiency [16].

This section illustrated the design of flyback converters and different control schemes for PV systems in the literature survey. This paper aims on designing SS and QR flyback converters for a solar panel. Linear and nonlinear control systems are developed to control the output voltage of these converters for the load requirements of PV systems. The following sections show the design and simulation results of the designed flyback converters as open loop and closed loop (using control techniques) systems. This work summarizes and

outlines the study analysis and system performance of the proposed PV systems with respect to different conditions, such as sun radiation level and different load values, which were not reported in the literature.

3. DESIGN OF FLYBACK CONVERTERS

The flyback converters are by far the most used topology for low-output power applications where galvanic isolation and/or multiple outputs are required since they have a low system cost and are simple to build. They are used as the major source of power for devices and appliances with reduced power. The selection of mode/type of switching depends on several factors including power, performance, shape factor, development time, application, etc. [17]. Fixed frequency (FF) and QR are the two basic operating switching modes. FF switches operate either in DCM or CCM, although the QR mode is based on variable switching frequency. MATLAB/Simulink is used to model and simulate these flyback converters as open loop systems, where the input source (V_{in}) mimics the output of a solar panel (17 V). The proposed flyback converters - without control systems (open loop) - are designed to output 24 V that can be used to power electronic systems, charge batteries, and feed loads/grid via inverters, as shown in Fig. 1. The following subsections illustrate the design of SS and QR flyback converters to output 24 V from the solar panel (17 V) without controlling the duty cycle or switching frequency. The simulation results of this section represent the performance of these converters when no control systems are used, just the switching frequency and duty cycle are fixed for the design requirements, i.e., this is an open loop system. The components of these converters are calculated with respect to the design requirements, a resistive load (as an example for dummy load) is used for the open-loop systems for the required output (24 V) as described below.

3.1. SS Flyback Converter

Fig. 2 shows the circuit diagram of the SS flyback (based on FF mode), which consists of a MOSFET switch (Q), an isolated transformer (primary winding (L_p), secondary winding (L_s), diode (D), magnetizing inductance (L_m) and capacitor filter (C_o).

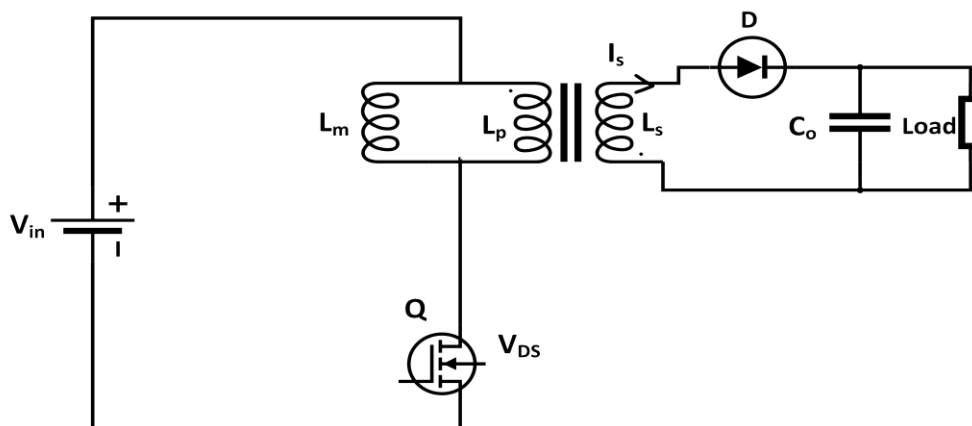


Fig. 2. Circuit diagram of the SS flyback converter.

As the Q is switched on, V_{in} is applied to the primary winding. At this period, the secondary winding is polarized oppositely to the primary inductor and thus the diode blocks the applied voltage because it will be an open circuit. There is no transfer of energy between input and output. When Q is turned-off, stored energy at the air gap and magnetic core is transferred to the secondary winding, and load is fed by the L_s . The I_s (secondary current) discharge linearly over resistive load [18].

During the Q on time, there is a fixed voltage across the L_p that can be obtained as [18]:

$$L_p = \frac{(V_{in-min}-1) \times T_{on-max}^2 \times V_{in-min}}{2.5 \times P_{o-min} \times T} \quad (1)$$

where, V_{in-min} is minimum input voltage, T_{on-max} is maximum turn-on time, P_{o-min} is minimum output power, and T is the period cycle of the switching frequency (f_s) for the switch. The turn ratio between the transformer primary side and secondary side is equal to [19]:

$$N = \frac{N_p}{N_s} = \frac{V_{in}}{V_o} * \frac{D_{max}}{1-D_{max}} \quad (2)$$

where D_{max} is the maximum duty cycle of SS flyback converter. According to simulations setup and design requirements, the main parameters of the proposed SS flyback design are $V_{in} = 17$ V, $V_o = 24$ V, $f_s = 150$ kHz, $N_p/N_s = 20:31.55$, $L_m = 1$ mH, $C_o = 22000$ μ F, $D_{max} = 0.5$.

Fig. 3(a) shows the simulation results of the output voltage (24 V), where the settling time (t_s) is 0.01 s. Peak to peak output ripple voltage is about 0.6 mV, as shown in Fig. 3(b). A 6.3 Ω is used as a resistive load, which results to output current of 3.81 A_{RMS} and peak-to-peak ripple of 8 mA, as shown in Fig. 4(a). The output voltage and current profiles show low ripple values because of the high value of the output filter capacitor ($C_o = 22$ mF), which should be considered in the experiment work (for the physical dimension and cost), where the output ripple value depends on the capacitor value. The input and output powers are 107.6 W and 91.85 W (shown in Fig. 4(b)), respectively. Consequently, the efficiency of this design SS flyback is about 85.3%.

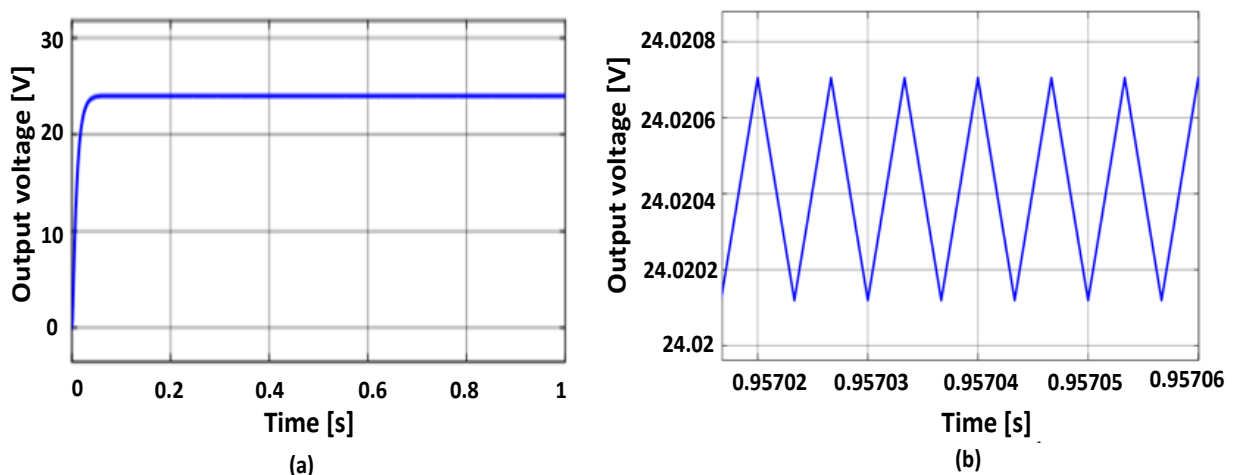


Fig. 3. Simulation results of the SS flyback (open loop): a) output voltage; b) peak to peak output ripple voltage.

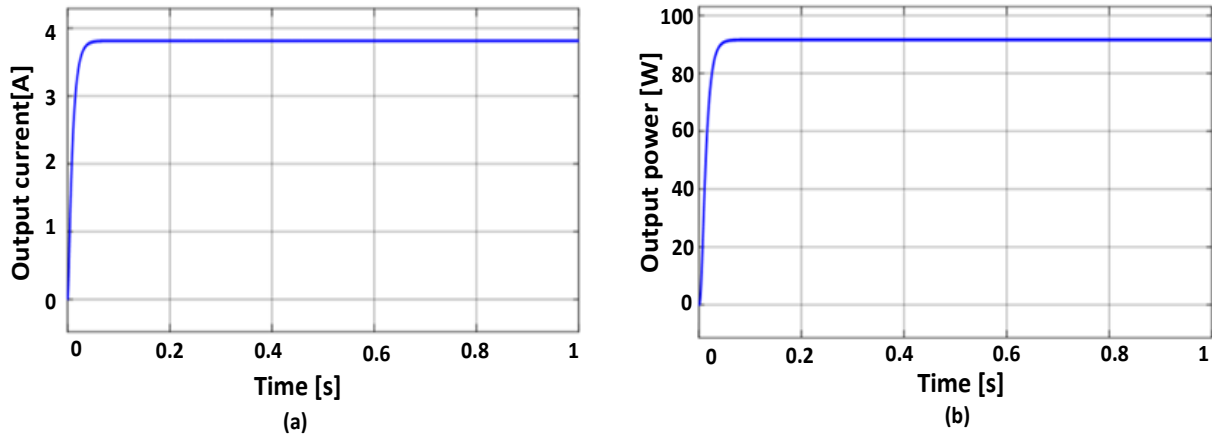


Fig. 4. Simulation results of SS flyback (open loop): a) output current; b) output power.

3.2. QR Flyback Converter

The QR flyback is essentially a DCM flyback with a valley switching on. It is also recognized as a variable frequency or valley switching flyback and is widely used in low-power switch mode power supply applications such as charger, adapter, and auxiliary power supply [17]. This subsection includes the approach in designing QR flyback with design equations. Fig. 5 shows the circuit diagram of QR DC-DC flyback that consists of a MOSFET switch, clamp capacitor C_c , transformer winding T_r , leakage inductance L_{lk} , magnetizing inductance L_m , transformer primary inductor L_p , transformer secondary inductor L_s , output filter capacitors C_o , secondary side diode D and the load. QR flyback converter topology seems like a modification of the standard flyback.

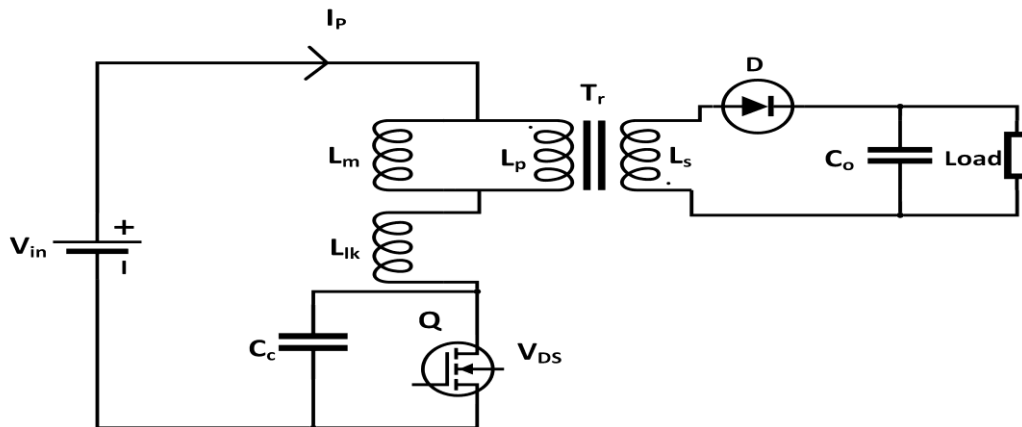


Fig. 5. Circuit Diagram of QR flyback converter.

Once the switch is turned on, the input voltage is forced onto the transformer primary, and the magnetizing inductance L_m starts to charge. As a consequence, the capacitor C_c is discharged, and the voltage across C_c is such that diode D is reverse biased. As a result, the transformer continues to be magnetized, but only because of the voltage of the main transformer winding. When the switch is turned off, the current no longer flows through the switch but flows through the output capacitance C_o and diode D . The transformer starts demagnetizing itself and the stored energy is transferred to the load when the secondary diode tends to conduct. As the secondary current drops to zero, both the windings of the

transformer are decoupled so that the reflected output voltage NV_o and the primary voltage are no longer equal to each other. The diode D becomes forward biased if the voltage over the clamp capacitor (V_c) is high enough. The conduction of the D depends on the resonant interaction between the C_c and the equivalent inductance. The turns ratio (N) of the transformer winding T_r is calculated from the peak duty cycle (D_{pk}) as [11]:

$$N \geq \frac{V_{in}}{V_o} \left(\frac{1}{D_{pk}} - 1 \right)^{-1} \quad (3)$$

The value of the clamp capacitor can be determined by considering the energy balance between the C_c and the L_{lk} , as almost all of the leakage energy is eventually transferred to the clamp capacitor. This energy balance can be expressed as [11]:

$$\frac{1}{2} C_c * \delta V_c^2 = \frac{1}{2} L_{lk} * I_{P-pk}^2 \quad (4)$$

where, δV_c is the maximum voltage rise across the C_c and I_{P-pk} is the peak primary current. The resonant period, switch turn-on time, and turn off-time can be determined from the total time ($T_s(t)$) - for any particular switching interval - that can be given by [11]:

$$T_s(t) = T_{on}(t) + T_{do}(t) + \frac{T_{qr}}{2} = \frac{I_{P-pk}(t) * L_m}{V_{in}} + \frac{I_{P-pk}(t) * L_m}{NV_o(t)} + \frac{T_{qr}}{2} \quad (5)$$

where $T_{do}(t)$ is the secondary diode conduction time and T_{qr} is the primary switch that needs to be turned on after a time of the resonant period. The switching frequency (f_s) can be obtained as:

$$f_s = \frac{1}{T_s} = \left(I_{P-pk}(t) * L_m \left(\frac{1}{V_{in}} + \frac{1}{NV_o(t)} \right) + \frac{T_{qr}}{2} \right)^{-1} \quad (6)$$

The peak duty cycle and turns ratio are interrelated for a fixed voltage gain if the converter is operated in DCM. With respect to these derived equations of the QR flyback and design requirements, we find that the D_{pk} and C_c are equal to 0.6 and 0.12 μF , respectively. The recommended range of the switching frequency for the QR flyback is from 80 kHz to 200 kHz [11], the f_s was set as 150 kHz. The other parameters are defined as ($V_{in} = 17 \text{ V}$, $V_o = 24 \text{ V}$, $N_p/N_s = 1:7.8$, $L_m = 12.8 \mu\text{H}$, $L_{lk} = 0.4 \mu\text{H}$, $C_o = 500 \mu\text{F}$, $R = 6.3 \Omega$ (resistive load)).

The output voltage of the QR flyback design stabilizes after 10 ms. The peak-to-peak ripple is 15.8 mV, as shown in Fig. 6. The output current equals 3.811 A_{RMS} and the peak-to-peak ripple is 2.5 mA, as illustrated in Fig. 7(a). The system efficiency of the QR design is 88.9%, as the input and output powers are 102.8 and 91.48 W as shown in Fig. 7(b).

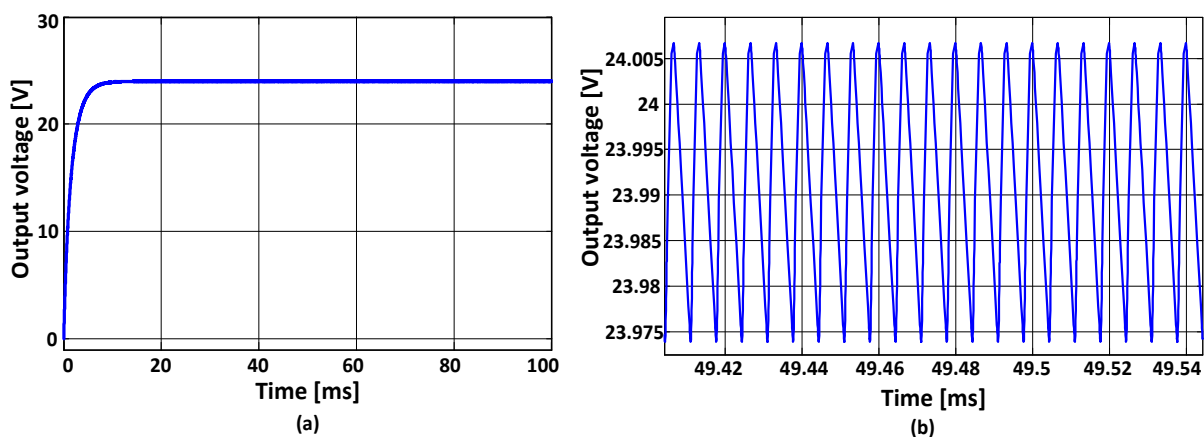


Fig. 6. Output voltage of QR flyback (open loop): a) zoomed in; b) full waveform.

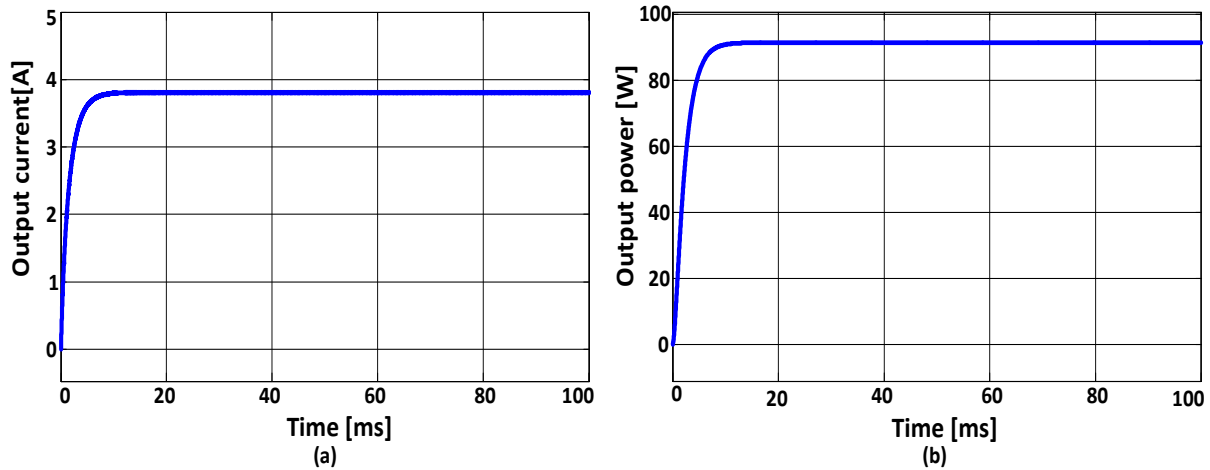


Fig. 7. Simulation results of QR flyback (open loop): a) output current; b) output power.

4. CONTROL SYSTEM DESIGNS FOR FLYBACK CONVERTERS

Control systems were designed to control and regulate the output voltage of the proposed converters to 24 V that can be used to provide power to electronic circuits, charge batteries, etc. The control system consists of PID/FLC controller and PWM, where the output of the controller is compared with a sawtooth signal to generate PWM. The V_{P-P} of the sawtooth signal for the SS and QR flyback converters are configured as 1 V and their frequency values are 5 and 150 kHz, respectively. Fig. 8 illustrates the block diagram of the closed loop control system for the flyback converters, whereas the desired output voltage (reference signal to the PID/FLC) is set to 24 V_{DC} for the loads. The following subsections illustrate the control design systems and the simulation results for the SS and QR flyback converters that were designed in the previous section. The previous section included the simulation results of the open loop systems that showed to have limitations of their performance when the design constraints, conditions, and load change. The following subsections illustrate the simulation results of these converters using the proposed controllers while the source voltage (V_{in} from the solar panel) is varying, and the load has different values. The change in the solar radiation level is represented by varying the output voltage from a solar panel (V_{in}), which is used to simulate the system performance of SS and QR flyback converters. The following simulation setups are conducted using either resistive or complex loads depending on the control system designs.

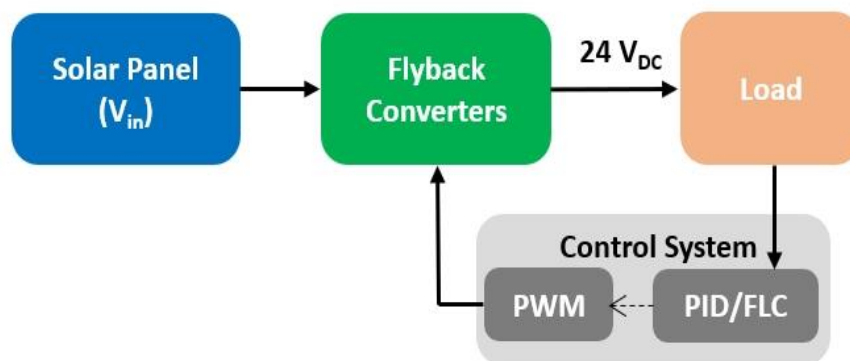


Fig. 8. Block diagram of the closed loop control system for the flyback converters.

4.1. PID Controller for Flyback Converter

PID controller consists of the proportional (P), integral (I), and derivative (D) parameters that determine: i) the reaction to the current error, ii) the reaction based on the sum of recent errors and iii) the reaction to the rate at which the error has been changing. The main purpose of using the PID controller is to obtain a constant output voltage for input (V_{in}) disturbance and different conditions. This can be achieved by directly tuning the PID gains. In our work, the output signals of the PID controller ($u(t)$) of the SS and QR flybacks were compared with a sawtooth signal to output square pulses (PWM) for the switch. The reference signal of the system is set to 24 V. Table 1 shows the effect of the PID gains for the output response, which is used to tune the PID controller [20, 21]. It was found that the PI controller is the best candidate, as it achieved a faster response than using the derivatives with respect to the plant model (SS & QR models). The PI gains were tuned as shown in Table 2.

Table 1. Effects of changing PID parameters.

Gain	Rise time	Overshoot	Settling time	Steady-state error	Stability
K_P	Decrease	Increase	Small change	Decrease	Degrade
K_I	Decrease	Increase	Increase	Eliminate	Degrade
K_D	Minor change	Decrease	Decrease	No effect	Improve

Table 2. Parameters of PI controller.

Gain	SS	QR
K_P	0.35	0.033
K_I	19.43	14.72

The system was simulated when the input voltage was constant and varying at different values. Fig. 9(a) shows the output voltage of SS flyback converter with no overshoot when the input voltage is 17 V (from a solar panel), which stabilizes over 0.12 s.

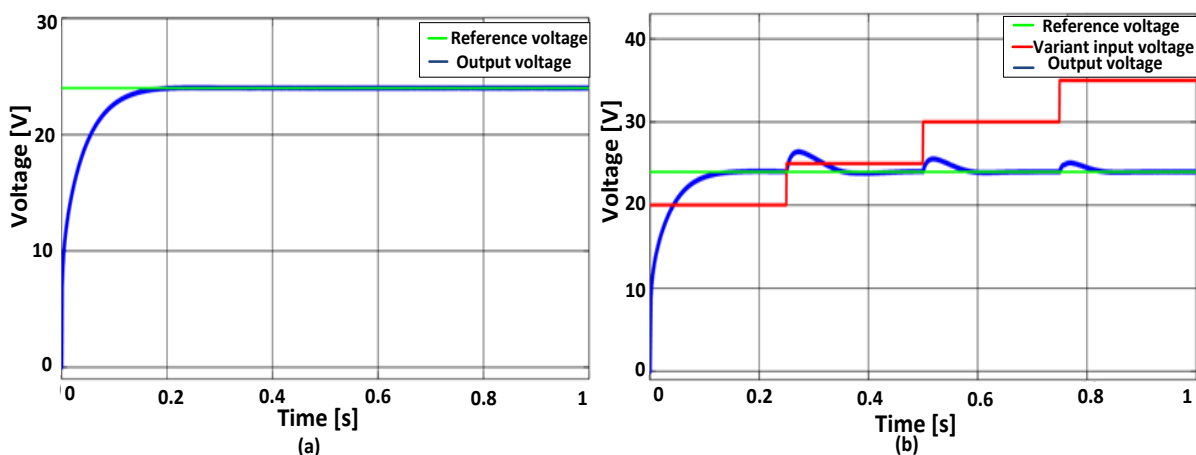


Fig. 9. Output voltage of SS flyback using PID when V_{in} is: a) a constant; b) variant.

The output current equals 4.133 A_{RMS} and the peak-to-peak ripple is 0.5 mA, as illustrated in Fig. 10(a). The system efficiency of the SS flyback using PID when V_{in} equals 17 V is 90.18%, as the input and output powers are 110 and 99.2 W (shown in Fig. 10(b)),

respectively. The output power and efficiency of the SS flyback improve using PID than open loop system by 2%. The PV system is simulated using a variant input source, which mimics the output voltage from the harvested power from a solar panel. This harvested power would be changing with respect to sun radiation levels and other variables. The input voltage (V_{in}) is set to 20, 25, 30, and 35 V at 0, 0.25, 0.5 and 0.75 s, respectively. The maximum overvoltage and settling time (0.27 s) occurs when the input voltage changes to 25 V, as shown in Fig. 9(b).

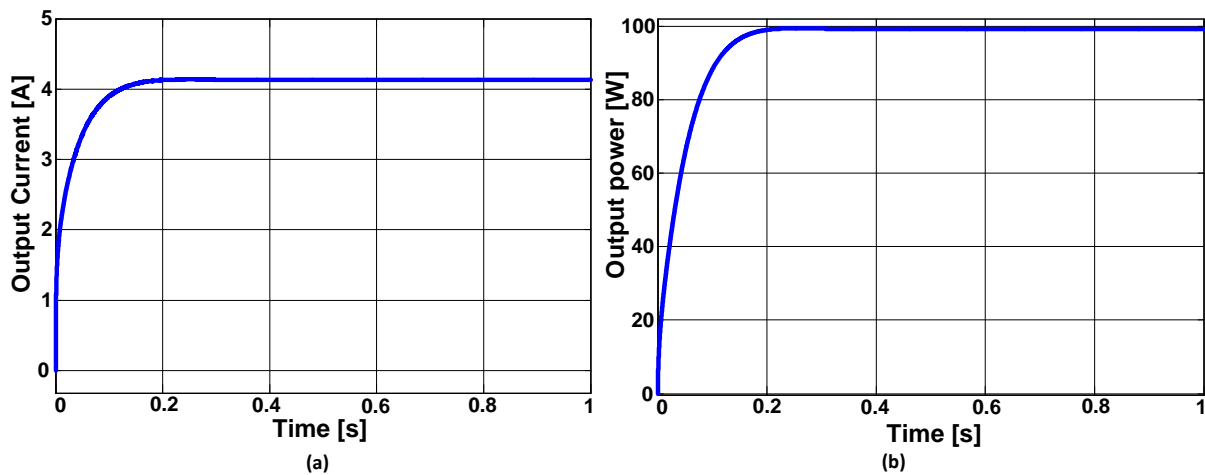


Fig. 10. Simulation results of SS flyback using PID: a) output current; b) output power.

Fig. 11(a) shows the output voltage of QR flyback, with no overshoot using input 17 V, which stabilizes after 10 ms. As shown in Fig. 12(a), the output current is 4.098 A_{RMS} and its peak-to-peak ripple is 1.8 mA. The input and output powers are 105.5 and 98.29 W (shown in Fig. 12(b)), respectively. Consequently, the efficiency of this QR flyback using PID when V_{in} is constant at 17 V equals 93.17%. The output power and efficiency are improved using the PID control system as well. Fig. 11(b) illustrates the output voltage when the variant input source is used as 20, 25, 30, and 35 V at 0, 25, 50, and 75 ms (same conditions for SS flyback converter), respectively. It is found that the maximum overshoot of voltage occurs at settling time of 27 ms when V_{in} changes to 25 V.

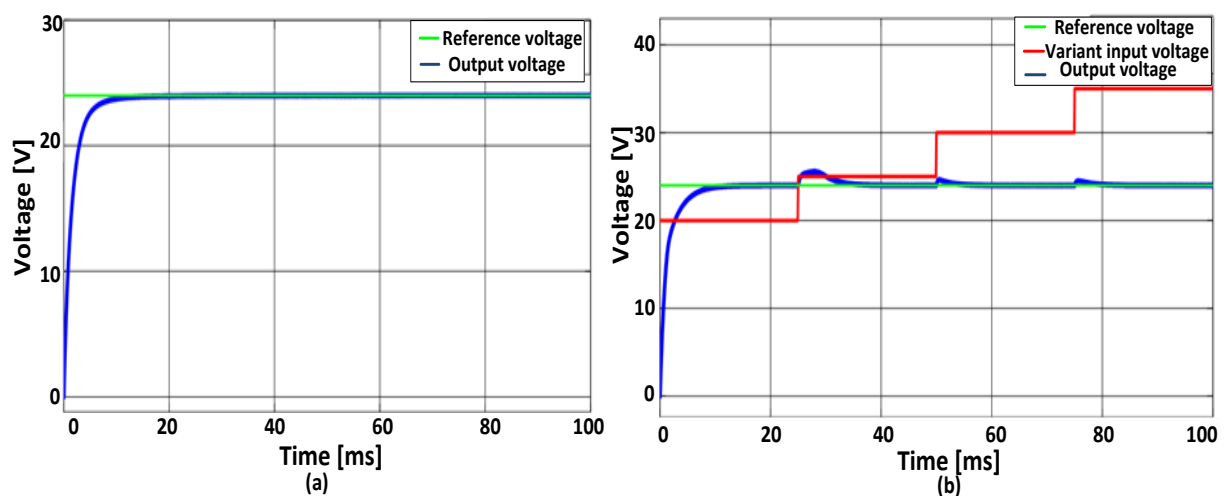


Fig. 11. Output voltage of the QR flyback using PID for: a) constant V_{in} ; b) variant V_{in} .

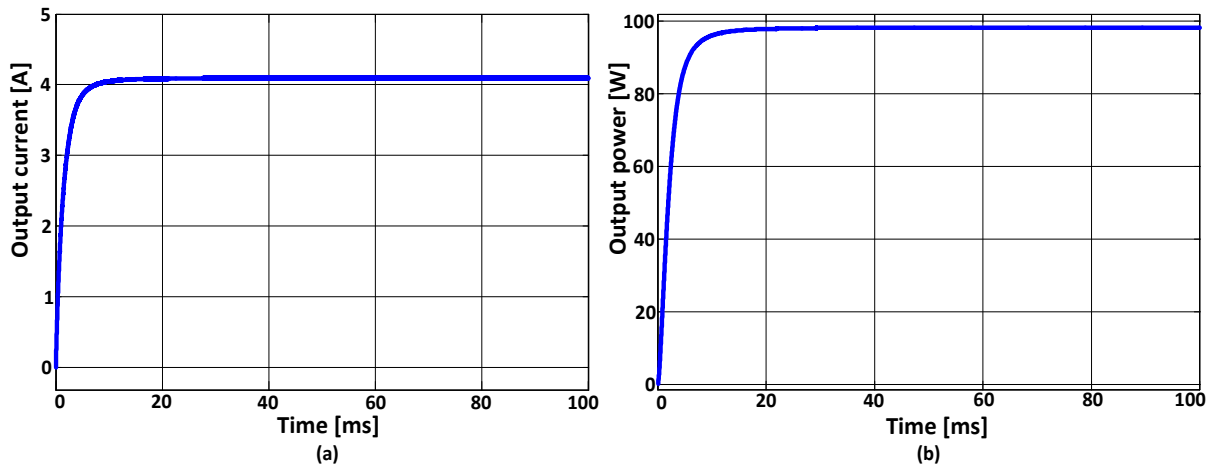


Fig. 12. Simulation results of QR flyback using PID: a) output current; b) output power.

4.2. FLC for Flyback Converter

The FLC is a nonlinear control system that provides more efficiency than a linear control system. Fig. 13 shows the block diagram of FLC stages with two inputs which are error (E) and the change in error (E^*). The FLC consists of fuzzification, interface engine and defuzzification. The fuzzification is the process of converting the crisp input variables into a membership function (linguistic variables). The interface engine is based on fuzzy rules, which store knowledge about the operation of the process of the domain. The defuzzification process converts the fuzzy variables into crisp variables [21, 22]. Five linguistic variables for the FLC system are used, which are NL (Negative Large), NS (Negative Small), Z (Zero), PS (Positive Small), and PL (Positive Large). Table 3 shows the fuzzy rules that are formulated by assigning relationship between fuzzy inputs and outputs. Fig. 14 depicts the surface view of the designed FLC rules.

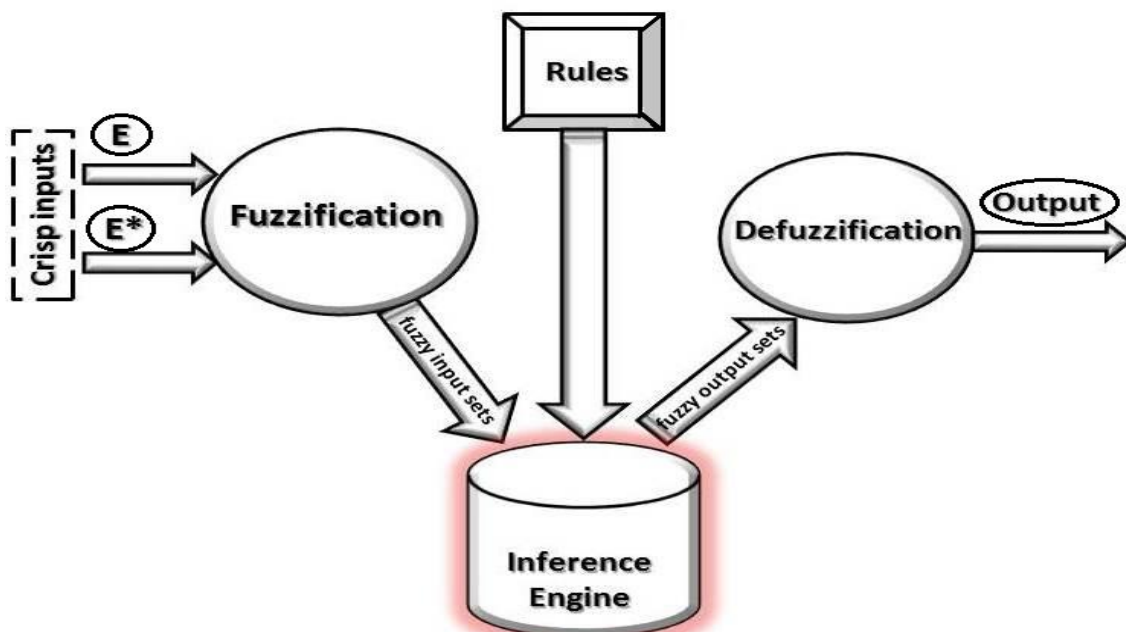


Fig. 13. Block diagram of FLC stages.

Table 3. Rules of the FLC.

E* \ E	NL	NS	Z	PS	PL
NL	NL	NL	NS	NS	Z
NS	NL	NS	NS	Z	PS
Z	NS	NS	Z	PS	PS
PS	NS	Z	PS	PS	PL
PL	Z	PS	PS	PL	PL

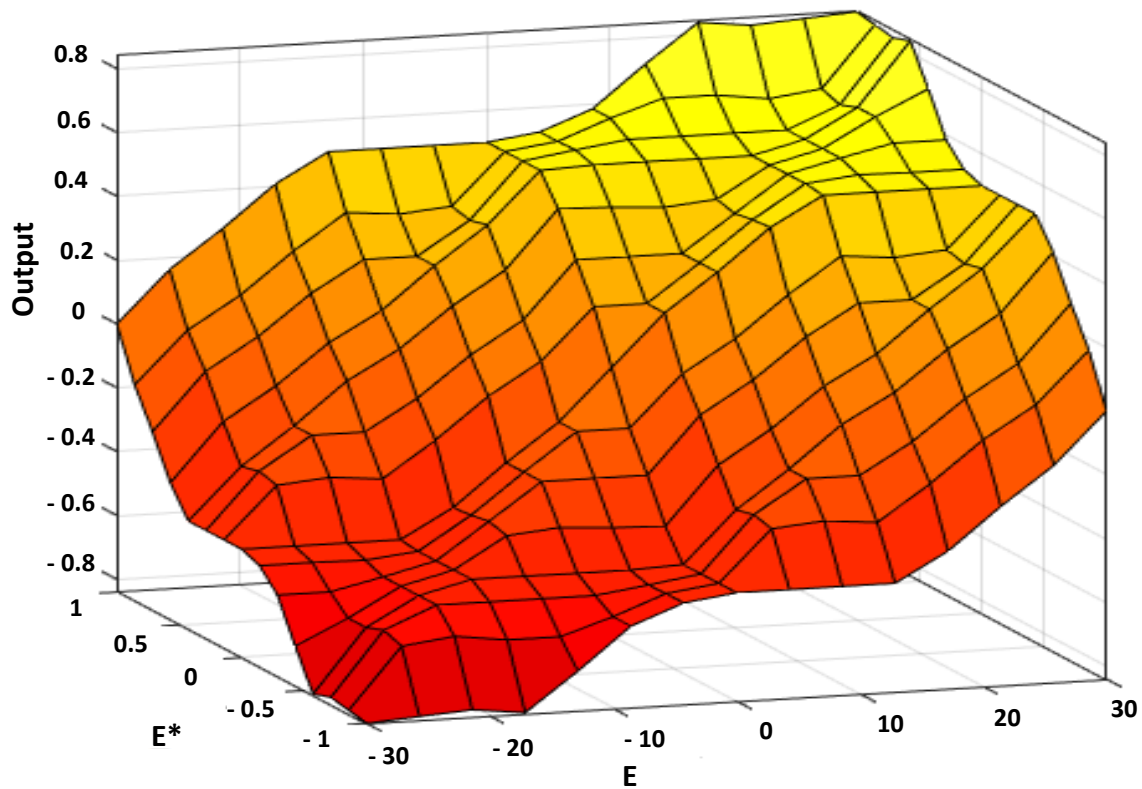


Fig. 14. Surface view of FLC rules.

The proposed SS and QR flyback converters are simulated using fuzzy libraries of MATLAB/Simulink. It is found that the output voltage of SS flyback stabilizes at 24 V with zero output ripple voltage when the input voltage is a constant value (17 V). The settling time is about 0.04 s, as shown in Fig. 15(a). Fig. 16(a) shows that the output current is 5.5 A_{RMS} with zero ripple current. The input and output powers are 148 and 135 W (shown in Fig. 16(b)), respectively. Therefore, the efficiency of this SS flyback using FLC when V_{in} is constant at 17 V is 91.1%. The output current and power using the FLC (nonlinear controller) are better than PID (linear controller), where the efficiency is higher by 1.1%. For the different sun radiation levels and other temperature values, the output voltage of the SS flyback converter is almost constant at 24 V (without overvoltage) when the input voltage changes at different times and values, as illustrated in Fig. 15(b).

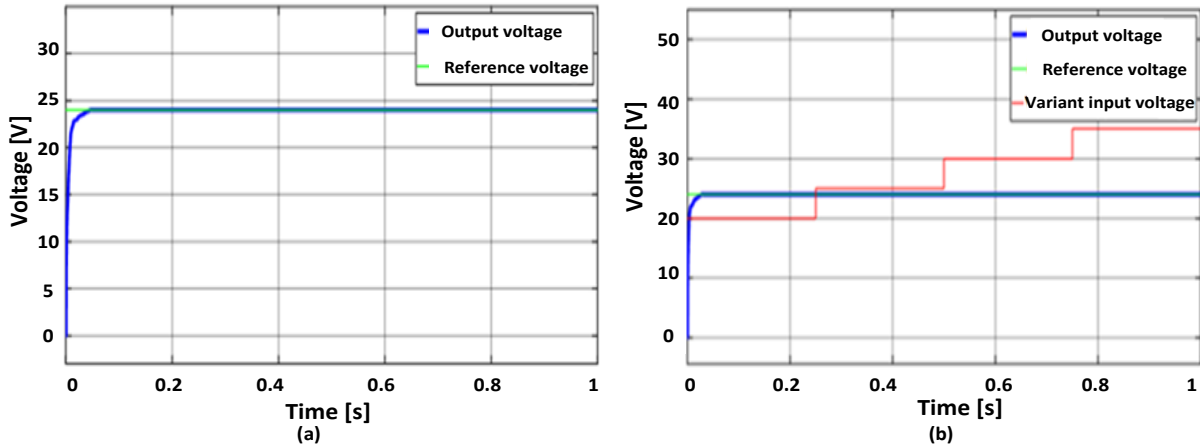


Fig. 15. Output voltage of SS flyback using FLC for: a) constant V_{in} ; b) variant V_{in} .

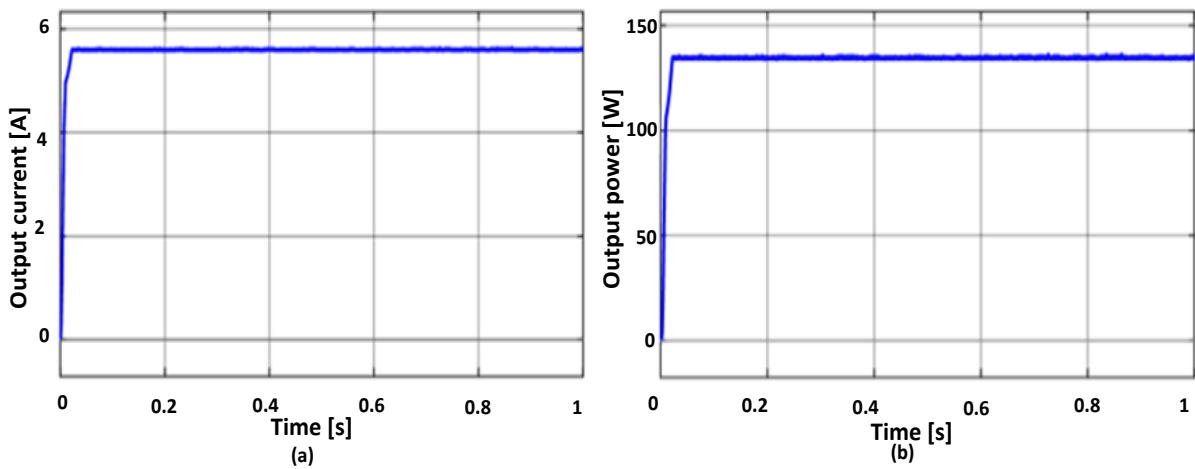


Fig. 16. Simulation results of SS flyback using FLC: a) output current; b) output power.

Fig. 17(a) shows the output voltage of QR flyback (24 V) when the input voltage is 17 V (as a constant value). The output voltage of the QR flyback converter using FLC stabilizes over 3 ms for the fixed V_{in} , as shown in Fig. 17(a). Fig. 18(a) shows the output current (6.8 A_{RMS}). The input and output powers are 175 and 164.7 W (shown in Fig. 18(b)), respectively, so the efficiency of this QR flyback using FLC when the V_{in} constant at 17 V is 94 %.

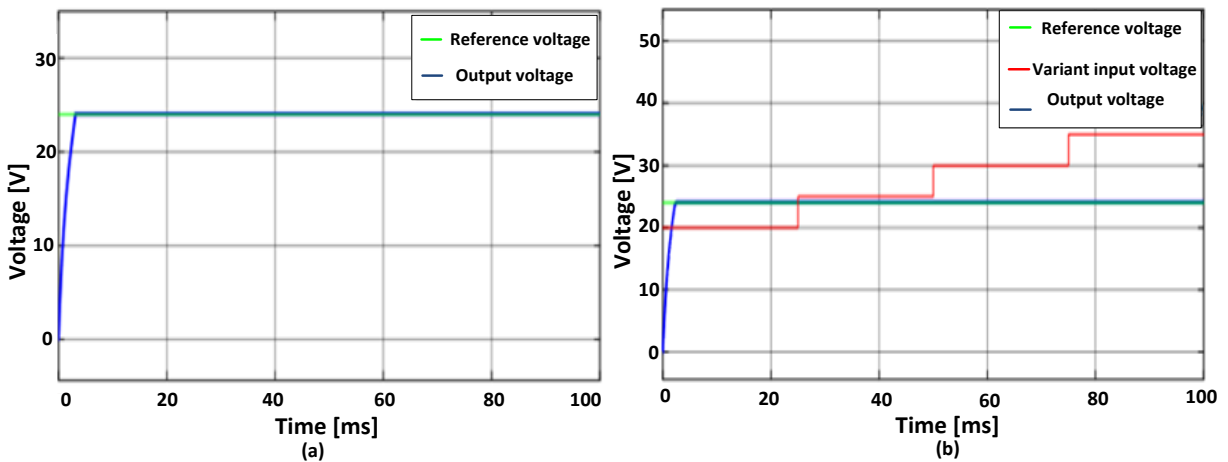


Fig. 17. Output voltage of QR flyback using FLC for: a) constant V_{in} ; b) variant V_{in} .

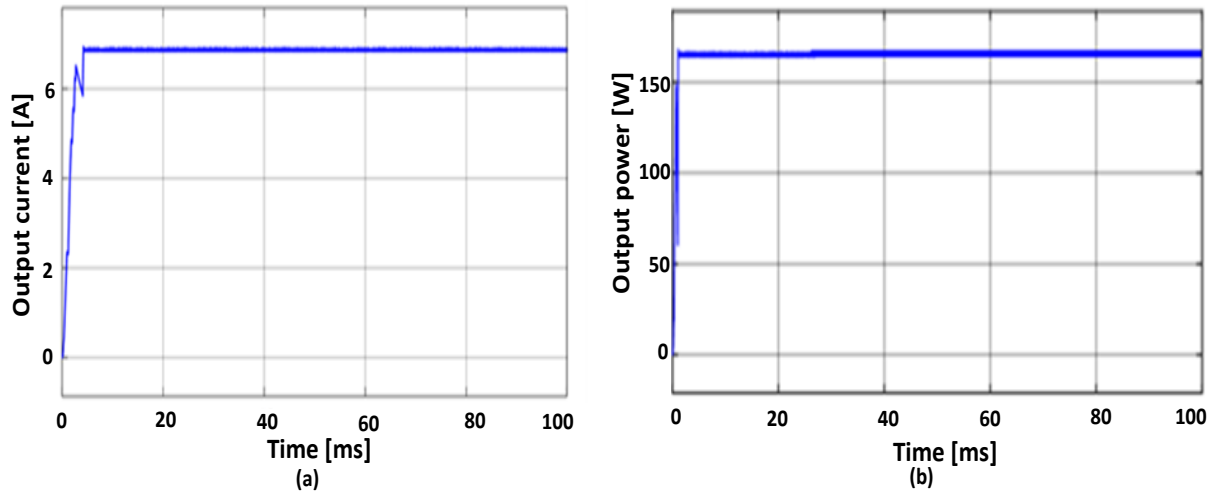


Fig. 18. Simulation results of QR flyback using FLC: a) output current; b) output power.

The efficiency and output current and power are using FLC are better than using PID and open loop systems. The output voltage is stable at 24 V while the V_{in} is varying at different times for the same conditions of the previous simulation setups, as illustrated in Fig. 17(b).

5. COMPARATIVE ANALYSIS OF THE FLYBACK CONVERTERS WITH PID AND FLC CONTROL TECHNIQUES

This work illustrated the design of SS and QR flyback converters that are based on FF and variable switching frequency. Table 4 lists the comparison of these modes [17, 23]. There are common advantages and disadvantages of SS and QR flybacks, as described as follows. The advantages of SS flyback are low cost, isolated, wide range of operation for DCM and CCM, and stability of its DCM mode because it does not have any zeroes in the right half-plane in the control loop. The disadvantages of SS flybacks are poor cross-regulation, challenging to compensate, large EMI filter, and limited from low to medium power levels. The pros of QR flybacks are lower switching losses (smaller EMI filter and high efficiency), low cost, isolated, wide range of operation, good transient response, and easy to compensate in DCM. The cons of QR flybacks are poor cross-regulation, limited to DCM, challenging EMI filter design, requiring a high output capacitance as it is operating in DCM region, and limited to low to medium power levels of switched-mode power supply (SMPS), such as charger, adapter, and auxiliary supply [3-16, 23].

Table 4. DCM, CCM, and QR flyback comparison.

Application parameter	DCM	CCM	QR
Operating frequency	Fixed	Fixed	Variable
Average efficiency	Low	High	The highest
Transformer design	Small	Big	Additional winding for valley detection.
Applications	Low power	Medium to high power	SMPS

Table 5 summarizes a comparison between closed loop controller techniques (PID and FLC) in a function of time response for SS and QR flyback. The main parameters used for comparison are ripple voltage, output power, efficiency (when the V_{in} was 17 V), overshoot (OS), delay time (t_d), peak time (t_p), settling time (t_s), and rise time (t_r). According to these results, the output power ratings and efficiency of the SS and QR flyback converters of the closed loop (PI and FLC systems) are higher than the open loop systems. These parameters approve that the FLC for SS and QR achieve a faster response than PI controller without overshoot while the sun radiation levels change (variant V_{in}). The output power values of the SS and QR using FLC are higher than open loop response by 45% and 65%, respectively.

Table 5. Comparison of closed loop for SS and QR flyback converters.

Mode	Ripple Voltage [mV]	Output Power [W]	Efficiency %	OS [% of 24 V]	t_d [ms]	t_p [ms]	t_s [ms]	t_r [ms]
PID-SS	4	99.2	90.2	10	5	25	134	71
FLC-SS	0	135	91.1	0	2	NA	47	9
PID-QR	16.4	98.3	93.2	6.67	1	2.67	7.58	3
FLC-QR	0	164.7	94	0	1	NA	3.1	2

It is found that the FLC (nonlinear) system was able to achieve the required voltage of 24 V smoothly at different conditions (load and variant input voltage from different sun radiation levels). The PID control system for the SS & QR flyback converters showed limitations for different input values (V_{in}) because of its linear operation. It is noticed that the QR flyback converter is better in terms of efficiency, output power, and transient response than the SS flyback.

6. CONCLUSIONS

This paper has illustrated and discussed the design of control systems for SS and QR flyback converters for a solar panel that has an output voltage of around 17 V. The proposed flyback converters are designed to output 24 V that can be used to power electronic systems, charge batteries, and feed loads/grid via inverters. MATLAB/Simulink was used to model and simulate the design of SS and QR flyback converters, where open loop and closed loop (PID and FLC) control systems are derived according to operation and equations of each converter. The designed flyback converters and their control systems were simulated for various conditions of PV applications, such as different sun radiation levels (variant V_{in}), and different loads. The responses of the SS and QR flybacks using PID and FLC are compared and analyzed for voltage regulations under these different conditions. It is observed that the FLC control technique for the SS & QR flybacks yields better transient and dynamic response than the PID control system due to its nonlinearity behavior. The simulation results showed that the maximum efficiency was 94% for the QR flybacks and the fastest response (settled over 3.1 ms) when the FLC was used because of its nonlinearity. The QR flyback converters provided higher power ratings than SS flyback converters. Based on the obtained results and the conducted analysis, the SS flyback converter is recommended for the low power level (such as LED lighting applications), and the QR for SMPS applications.

Conflict Of Interest Statement: The technology, products, views, and opinions expressed by the author are solely theirs, and are in no manner associated with, endorsed by, or attributable to Genesis Robotics and Motion Technologies, LP, or its affiliates.

REFERENCES

- [1] M. Fakhry, M. Saber, M. Eltantawi, S. Kaddah, B. Badr, "Design and analysis of controlled SEPIC and LLC converters for photovoltaic systems," *International Journal of Engineering Applied Sciences and Technology*, vol. 5, no. 8, pp. 54-63, 2020.
- [2] IEA, *Global Energy Review 2019*, IEA, Paris, 2020. <<https://www.iea.org/reports/global-energy-review-2019>>
- [3] K. Raghavendra, K. Zeb, A. Muthusamy, T. Krishna, S. Prabhudeva Kumar, D. Kim, M. Kim, H. Cho, H. Kim, "A comprehensive review of DC-DC converter topologies and modulation strategies with recent advances in solar photovoltaic systems," *Electronics Journal*, vol. 9, no. 1, pp. 1-42, 2019.
- [4] J. Gowrishankar, E. Kaliappan, D. Fathema Farzana, G. Chidambarathanu, K. Karthick, "Modeling of PV array for DC-DC flyback converter with asymmetrical output voltage," *International Journal of Engineering and Advanced Technology*, vol. 8, no. 6S3, pp. 1406-1409, 2019.
- [5] G. Chu, H. Wen, L. Jiang, Y. Hu, X. Li, "Bidirectional flyback based isolated-port submodule differential power processing optimizer for photovoltaic applications," *Solar Energy*, vol. 158, pp. 929-940, 2017.
- [6] U. Yilmaz, I. Kiracy, "PV system incremental conductance MPPT method applied flyback converter under variable temperature and irradiance," *European Journal of Technic*, vol. 6, no. 2, pp. 87-95, 2016.
- [7] M. Nasir, H. Khan, A. Hussain, L. Mateen, N. Zaffar, "Solar PV-based scalable DC microgrid for rural electrification in developing regions," *IEEE Transactions on Sustainable Energy*, vol. 9, no. 1, pp. 1-9, 2018.
- [8] A. Sharma, S. Singh, "Flyback-forward converter for solar based application," *International Journal of Advanced Research in Electrical, Electronics and Instrumentation Engineering*, vol. 5, no. 5, pp. 3600-3607, 2016.
- [9] J. Lee, T. Liang, J. Chen, "Isolated coupled-inductor-integrated DC-DC converter with non-dissipative snubber for solar energy applications," *IEEE Transactions on Industrial Electronics*, vol. 61, no. 7, pp. 3337-3348, 2014.
- [10] Z. Chen, Q. Zhou, J. Xu, "Coupled-inductor boost integrated flyback converter with high-voltage gain and ripple-free input current," *IET Power Electronics*, vol. 8, no. 2, pp. 213-220, 2015.
- [11] A. Mukherjee, *Single-Stage Flyback Micro-Inverter for Solar Energy Systems*, Electronic Thesis and Dissertation, University of Western Ontario, London, Canada, 2013.
- [12] Y. Zhou, *Design and Implementation of a PV Converter for DC Microgrid with Fast and Accurate MPP Tracking Strategy using Boundary Controller*, MSc Thesis, Department of Electrical and Computer Engineering, University of Manitoba, 2017.
- [13] S. Zengin, M. Boztepe, "Evaluation of two-stage soft-switched flyback micro-inverter for photovoltaic applications," *8th International Conference on Electrical and Electronics Engineering*, pp. 92-96, 2013.
- [14] S. Ansari, J. Moghani, "Soft switching flyback inverter for photovoltaic AC module applications," *IET Renewable Power Generation*, vol. 13, no. 13, pp. 2347-2355, 2019.
- [15] G. Tan, J. Wang, Y. Ji, "Soft-switching flyback inverter with enhanced power decoupling for photovoltaic applications," *IET Electric Power Applications*, vol. 1, no. 2, pp. 264-274, 2007.

- [16] W. Xiong, *Multi-Stage Flyback Converter for Wide Input Voltage Range Applications*, United States Patent, 2017.
- [17] A. Saliva, *Design Guide for QR Flyback Converter*, Infineon Technologies North America, 2013.
- [18] N. Coruh, S. Urgun, T. Erfidan, "Design and implementation of flyback converters," *5th IEEE Conference on Industrial Electronics and Applications*, pp. 1189-1193, 2010.

- [19] S. Deshpande, N. Bhasme, "Modeling and simulation of microinverter with flyback converter for grid-connected PV systems," *International Journal of Electrical and Electronics Engineering Research*, vol. 7, no. 4, pp. 71-82, 2017.
- [20] B. Badr, W. Ali, "Nanopositioning fuzzy control for piezoelectric actuators," *International Journal of Engineering and Technology*, vol. 10, no. 01, pp. 50-54, 2010.
- [21] B. Badr, W. Ali, *Fuzzy Control for Nanopositioning Piezoelectric Actuators*, VDM Verlag Dr. Müller, Germany, 2011.
- [22] S. Modak, G. Panda, P. Saha, "Comparative study between PID-controller and fuzzy logic controller of a novel flyback converter," *International Journal of Advanced Research in Electrical, Electronics and Instrumentation Engineering*, vol. 4, no. 5, pp. 4540-4548, 2015.
- [23] L. Dinwoodie, "Exposing the inner behavior of a quasi-resonant flyback converter," *Texas Instruments Power Supply Design Seminar*, pp. 2-27, 2012.